

GAM and Broadband Turbulence Structure in OH and ECRH Plasmas in the T-10 Tokamak^{*})

Alexander V. MELNIKOV^{1,2)}, Leonid G. ELISEEV¹⁾, Sergey A. GRASHIN¹⁾,
Mikhail A. DRABINSKIY^{1,3)}, Philipp O. KHABANOV^{1,3)}, Nickolay K. KHARCHEV¹⁾,
Ludmila I. KRUPNIK⁴⁾, Alexander S. KOZACHEK⁴⁾, Sergey E. LYSENKO¹⁾,
Vitaly N. ZENIN^{1,3)} and HIBP Team⁴⁾

¹⁾National Research Centre 'Kurchatov Institute', Moscow, Russia

²⁾National Research Nuclear University MEPhI, Moscow, Russia

³⁾Moscow Institute of Physics and Technology, Dolgoprudny, Russia

⁴⁾Institute of Plasma Physics, KIPT, Kharkov, Ukraine

(Received 28 December 2017 / Accepted 4 July 2018)

Zonal flows and their high-frequency counterpart, the geodesic acoustic modes (GAMs) are considered as a possible mechanism of the plasma turbulence self-regulation. In the T-10 tokamak, GAM and broadband (< 200 kHz) turbulence of plasma potential and density have been directly studied by heavy ion beam probing from the plasma core to the edge. Regimes with Ohmic and auxiliary electron cyclotron resonance heating (ECRH) were studied ($B_t = 1.7\text{--}2.4\text{ T}$, $I_p = 140\text{--}250\text{ kA}$, $\bar{n}_e = (0.6\text{--}3) \times 10^{19}\text{ m}^{-3}$, $P_{\text{EC}} \leq 1.2\text{ MW}$) for the plasma with tungsten rail limiter. GAMs are more pronounced during ECRH, when the typical frequencies f_{GAM} were in the band 22 - 27 kHz for the main frequency peak and 25 - 30 kHz for the higher frequency satellite. Both GAM and satellite have uniform structure with constant frequencies over a wide radial extension, exhibiting the features of plasma eigenmodes. The main GAM peak has wider outer bound at the plasma edge than satellite. f_{GAM} follows the theoretical expectation $f_{\text{GAM}} \sim \sqrt{T/m_i}/R$ (for electron temperature at $r/a = 0.7$) for both OH and ECRH regimes in the wide temperature area, covering the whole operational limit of T-10. At the plasma periphery, the quasicohherent electrostatic mode with frequency 50 - 120 kHz coexists with GAM and satellite.

© 2018 The Japan Society of Plasma Science and Nuclear Fusion Research

Keywords: tokamak, electric potential, geodesic acoustic modes, broadband turbulence, heavy ion beam probe, quasi-coherent mode

DOI: 10.1585/pfr.13.3402109

1. Introduction

In the recent years tokamak plasma fluctuations attract the significant interest since their relevance to the properties of the turbulent transport. It is believed that zonal flows and their high-frequency counterpart, geodesic acoustic modes (GAMs) presents a mechanism of the turbulence self-regulation [1]. GAMs involving $m = 0$ component of the electrostatic potential and $m = 1$ component of the plasma pressure were first introduced in [2] within the ideal MHD model. The general properties of GAMs have been reviewed in [3]. Recently GAMs were intensively studied in a number of tokamaks and stellarators [4–6]. To analyse the temperature dependence of GAM, the following equations were used:

$$f_{\text{GAM}} = c_s/2\pi R, \quad (1)$$

where R is the major radius and the sound speed c_s is:

$$c_s = \sqrt{(T_e + T_i)/m_i}. \quad (2)$$

author's e-mail: Melnikov_AV@nrcki.ru

^{*}) This article is based on the presentation at the 26th International Toki Conference (ITC26).

In most of the experiments, GAMs were found to be an edge phenomenon [7], while this was often caused by the limitations of the used diagnostics. However, it has been recently found that GAM may be radially extended [8, 9]. Several experimental works show the radial variation of the GAM frequency [10]. However, other experiments suggest that the observed GAM fluctuations have constant frequency over some radial extent, limited by diagnostic capabilities [8, 11], presenting the structure of the radially extended eigenmode. So, the GAM radial structure is still an open question at the moment. It presents the challenge for the diagnostics to detect GAMs in the plasma core.

In the T-10 tokamak, the modes in the geodesic acoustic frequency range have been studied by the heavy ion beam probing (HIBP) [12, 13], correlation reflectometry and multipin Langmuir probes (MLP) [14]. Previously our measurement in outer zone at the low field side have shown that the mode frequency f^{exp} scales approximately as \sqrt{T} that confirms that these modes are induced by the geodesic compressibility and belong to the GAM type. These results were obtained with a conventional carbon limiter. One of

the goals of this work is to study the properties and radial structure of such modes in the whole radial range of T-10 from the plasma edge to the central region in the plasma with all-metal wall [15].

Electron cyclotron resonance heating (ECRH) is known as a powerful tool for the radially localized heating of the plasma electrons. Significant progress has been reported regarding the physical understanding of empirical actuators like ECRH core heating to avoid impurity accumulation as a potential showstopper for the development of fusion energy [16]. Recent advances in the HIBP [17, 18], opens the possibility to study plasma turbulence in a wide frequency range and in higher densities. The paper describes the recent observations of the properties of GAMs and broadband plasma turbulence in OH and ECRH plasma discharges limited by the rail tungsten limiter made by ITER technology [15].

2. Experimental Set-Up

Experiments in the T-10 circular tokamak ($R = 1.5$ m, $a = 0.3$ m), were performed with a reduced magnetic field $B_t = 1.7$ T, and current $I_p = 200$ kA, so the edge safety factor was $q(a) \sim 2.5$, while density evolves within the range $\bar{n}_e = (0.2 - 2.5) \times 10^{19} \text{ m}^{-3}$. The discharge scenario is shown in the Fig. 1. On top of that, the discharges with auxiliary ECR heating with the power P_{EC} up to 1 MW were studied. The main diagnostic to study plasma electrostatic turbulence in the core plasma of T-10 is HIBP. It uses Ti^+ ions with initial energy $E_{b1} = 200 - 300$ keV. HIBP is capable to measure the profiles of local plasma potential φ_{SV} in the Sample Volume (SV) from difference of primary and secondary energies: $\varphi = \varphi_{SV} = (E_{b1} - E_{b2})/e$, (e is the elementary charge) and relative density fluctuation \tilde{n}_{SV}/n_{SV} from the secondary beam current \tilde{I}_{tot}/I_{tot} in the frequency range < 500 kHz. The 5-slits energy analyzer allows us to get the local potentials in several spatial points (SVs) simultaneously, so to retrieve the electrostatic turbulence particle flux, as discussed in [19].

HIBP scans the plasma cross section by periodical variation of beam entrance angle to the plasma (scanning voltage U_{scan}) with period from 10 to 100 ms. Calculations of beam orbits have shown that HIBP is capable to observe the considerable part of plasma cross section $0.2 < \rho_{SV} = r_{SV}/a < 1$. For the experimental conditions, shown in Fig. 1, the plasma density is not very high ($n_{SV} < 2.2 \times 10^{19} \text{ m}^{-3}$), so one can neglect the path-integral effect [20] and suppose that the density fluctuation measurements are rather local.

Plasma potential and density signals were measured in a series of the reproducible discharges, with a sampling frequency < 1 MHz and radial resolution < 1 cm.

HIBP beam energy was changed from shot to shot, so various radial areas were observed. For the each beam energy, the sample volume position was periodically changed during ~ 10 ms by the scan of the beam entrance angle.

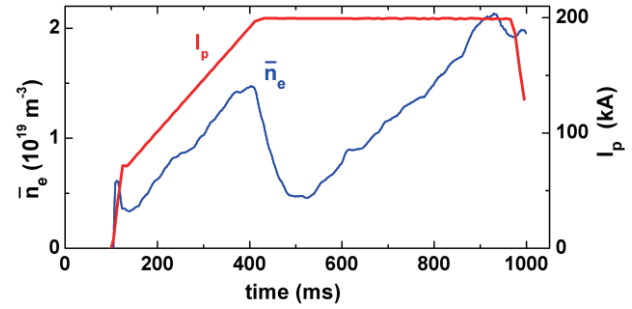


Fig. 1 The typical discharge scenario, which allows to look at the GAM and broadband turbulence in a density range $\bar{n}_e = (0.5 - 2.2) \times 10^{19} \text{ m}^{-3}$, #70991.

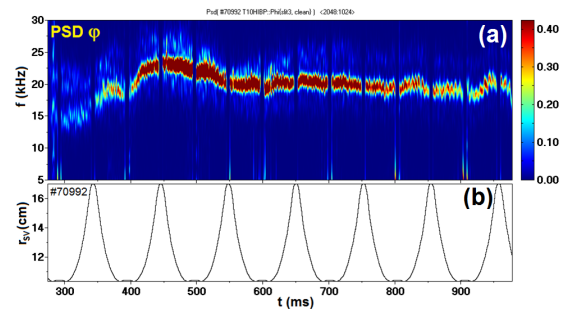


Fig. 2 (a) Power spectrogram of the plasma potential; (b) the time variation of sample volume position r_{SV} .

An example of the results, obtained in such experiment is shown in Fig. 2.

Figure 2 (a) shows the time evolution of the potential power spectral density (power spectrogram, PSD) in the low-frequency range, while Fig. 2 (b) shows the time variation of ρ_{SV} . The radial length of 1 cm has been passed during 1 - 3 ms, so it took from 1 to 3×10^3 samples, and forms the so-called “slow scan” with high temporal resolution. Then the Fourier power spectrograms were reconstructed with Hann sliding window, having a time-series (NFFT) $\sim 10^3$ samples per 1 ms, so providing the high temporal and spectral resolution.

For slow evolving processes, assuming the absence of the fast irregular changes during 1 ms, one may transfer the time dependence of the power spectra (PSD) to the radial spectra dependence. Figure 2 (a) shows that GAM is strongly dominating in the potential spectrogram. This holds for the whole observed radial range.

3. Experimental Results

3.1 Ohmic plasma

Potential power spectrograms from different radial areas were unified into a set presented in Fig. 3. This is a joint picture, covering the whole radial observation range for the regime under analysis. Each row of the matrix presents the radially resolved potential PSD, obtained for a specific energy E_{b1} . The upper row corresponds to the lower E_{b1} and

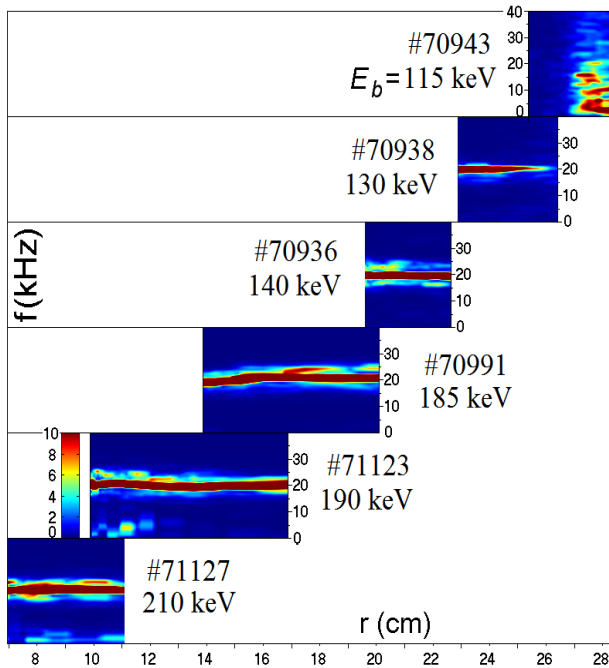


Fig. 3 The radial reconstruction of potential PSD for the series of identical shots with $B_t = 1.7$ T, $I_p = 220$ kA. Scans are chosen at density $\bar{n}_e = 1.0 \times 10^{19} \text{ m}^{-3}$.

the outer radial range. The radial ranges are not equal for each E_{b1} due to the peculiarities of the beam trajectories. For each pair of the neighboring spectrograms there is a radial area of the overlapping. Figure 3 shows that the spectrograms in the overlapping area are identical that proves the consistency of the measurements. The radial length of fragments is varied from 3 to 10 cm, depending on the beam energy.

Figure 4 shows the unified radial PSD over the whole observation area. It shows the uniform radial structure of GAM frequency $f_{\text{GAM}} = 20$ kHz. In addition, there is a satellite peak with a weaker power and frequency $f_{\text{sat}} = 24$ kHz, which also has a uniform radial structure. This radial uniformity of both peaks is consistent with the earlier observation, performed at low magnetic field $B_t = 1.55$ T [11]. Finally, one may see that GAM on T-10 presents the features of the radially extended or global eigenmode with a constant frequency over the plasma minor radius.

Figure 5 presents the radial profiles of the amplitude for GAM and satellite. Figure 5 shows that the GAM amplitude in potential is about 75 V, while for the satellite it is in a factor of 3 less, i.e. about 25 V.

The turbulence structure at the edge presents a specific interest. Figure 6 shows the density (a) and potential (b) PSD in the edge plasma. Inner part of the spectrogram shows the spectra, which are typical for the core plasmas. It contains the quasimonochromatic GAM excited in potential spectra at the frequency $f_{\text{GAM}} = 20$ kHz. Besides, it contains the quasicohherent (QC) mode [14] excited in

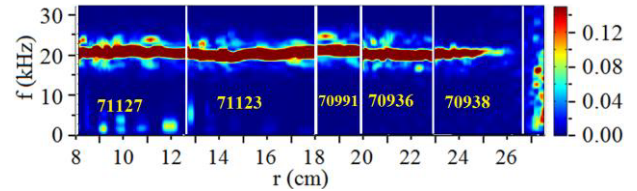


Fig. 4 The joint picture of the radial reconstruction of potential PSD (a. u.) for the series of identical shots with $B_t = 1.7$ T, $I_p = 220$ kA, $\bar{n}_e = 1.0 \times 10^{19} \text{ m}^{-3}$.

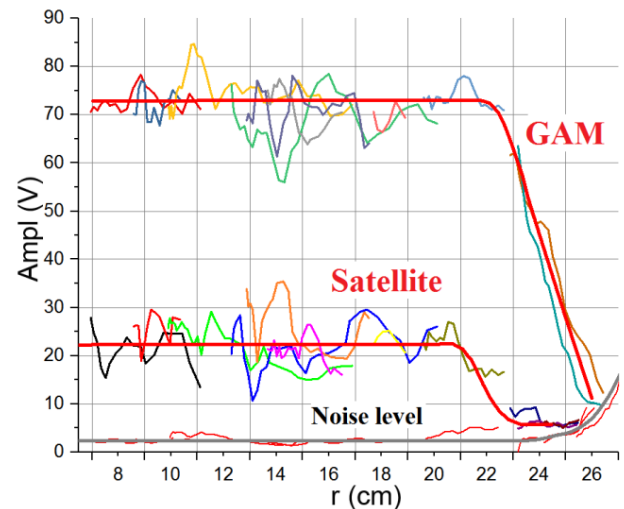


Fig. 5 The radial profiles of the amplitude of potential perturbation for GAM and satellite. Color curves are amplitudes taken from the shots of Fig. 3, red curves are best fits. Grey curve is the noise level. $B_t = 1.7$ T, $I_p = 220$ kA, $\bar{n}_e = 1.0 \times 10^{19} \text{ m}^{-3}$.

the frequencies from $f_{\text{QC}} = 50$ to 150 kHz. This mode is dominating in the density spectra. Radially outward part of the spectrogram shows the spectra, which are typical for the scrape-off layer (SOL) plasmas. It contains the specific low-frequency oscillations limited to 20 kHz.

The typical density spectra for the core plasma and SOL are presented in Fig. 7. They are taken from the shot, presented in Fig. 6. One may see the dominating low-frequency oscillations in SOL-like spectrum, while in the core the quasicohherent mode dominates. The SOL-like spectrum demonstrates fast decay in a range of about two decades, while the core spectrum presents significant values in the frequency range up to 200 kHz.

Remarkably, there is a sort of gap between the core and SOL types of spectra. In the gap there is no pronounced activity in the observed frequency range up to 300 kHz.

Figure 8 shows the spectrum observed by the Langmuir probe in SOL, which is similar to SOL spectrum shown in Fig. 7.

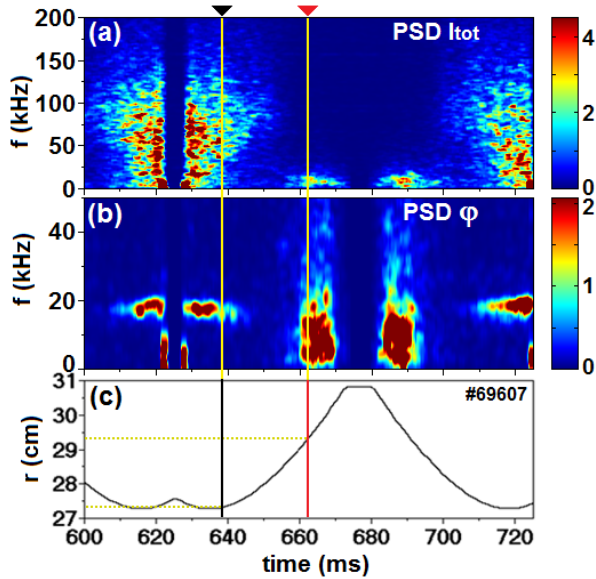


Fig. 6 The turbulence structure at the edge. (a) PSD of the plasma density with dominating QC peak, (b) PSD of plasma potential with dominating GAM peak, (c) evolution of the sample volume position; #69607, $B_t = 2.4$ T, $I_p = 210$ kA, $\bar{n}_e = 1.2 \times 10^{19} \text{ m}^{-3}$. Vertical lines show radial positions of spectra in Fig. 7.

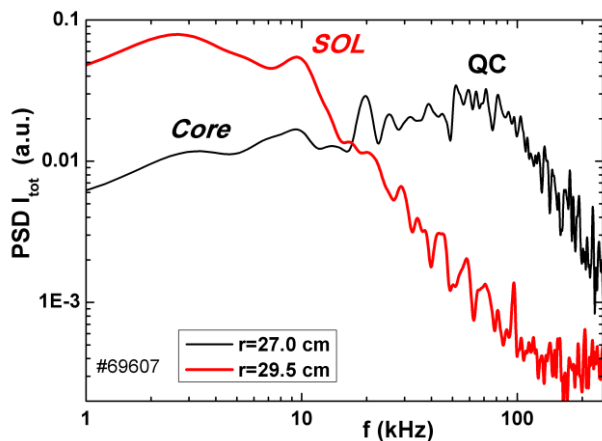


Fig. 7 Density turbulence power spectra in the core plasma (black) and in the SOL (red). QC peak is pronounced in the core spectrum.

3.2 ECRH plasma

ECRH presents an effective instrument to heat plasma electrons directly and locally. ECRH affects both GAM and QC. Figure 9(a) shows the plasma potential PSD of the discharge with auxiliary ECRH. Both GAM and satellite peaks became more intensive due to the ECRH. Time trace of the amplitude of the GAM-related activity, including both GAM and satellite, was estimated at the time-frequency domain, marked by polygonal region in Fig. 9(a). This time trace is presented in Fig. 9(c). Figure shows the fast increase of the amplitude in a factor of 2 from 75 V to 150 V followed by gradual decay. GAM fre-

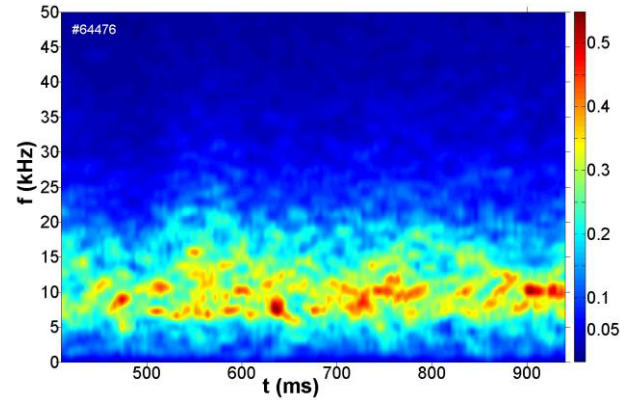


Fig. 8 Spectrogram of floating potential fluctuations measured by Langmuir probe in SOL ($r = 32$ cm); $B_t = 2.3$ T, $I_p = 220$ kA, $\bar{n}_e = 2 \times 10^{19} \text{ m}^{-3}$.

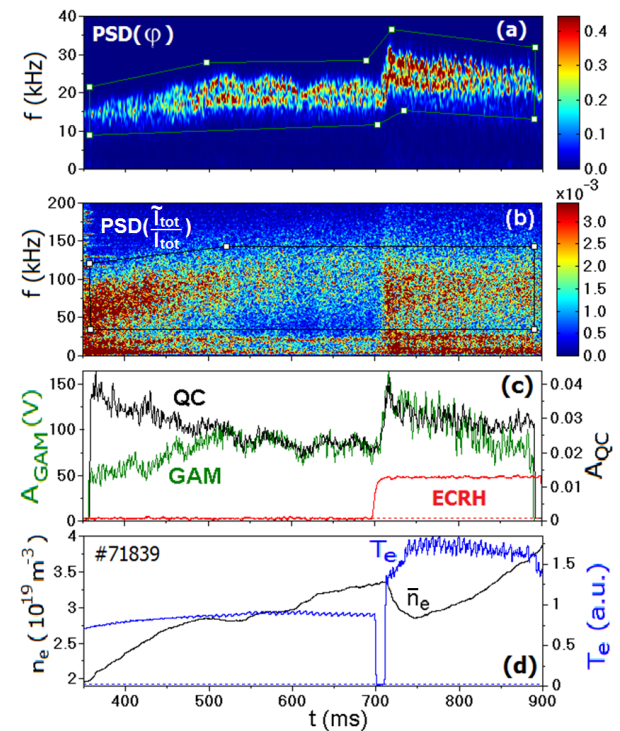


Fig. 9 Temporal evolution of GAM and QC mode in discharges with ECRH. Plasma potential (a) and density (b) power spectrograms; (c) amplitudes of GAM on potential (green) and QC on density (black) perturbations, integrated over the marked domains; (d) line-averaged density and electron temperature evolution. $B_t = 2.42$ T, $I_p = 250$ kA.

quency is evolving with T_e variation shown in Fig. 9(d) as predicted by the scaling (1). Figure 9(b) shows the plasma density power spectrogram. It shows the increase of the QC peak due to the ECRH. Time trace of the QC amplitude, estimated at the time-frequency domain, marked by polygon in Fig. 9(b) is presented in Fig. 9(c).

We see the fast increase of the amplitude in a factor

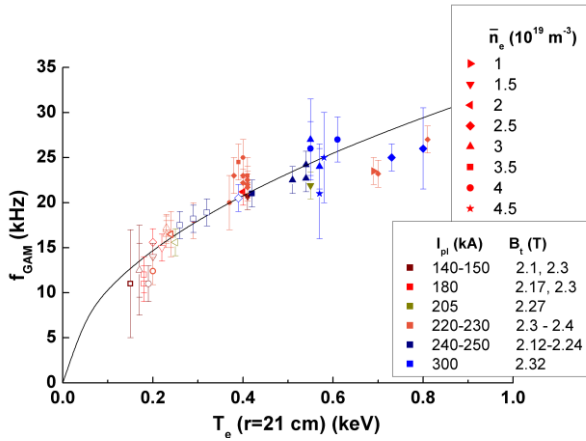


Fig. 10 GAM dependence on T_e . OH regimes - open symbols, ECRH regimes - closed symbols. The theoretical scaling (3) is shown by solid line.

of 2 from 2% to almost 4% followed by gradual decay. Remarkably, both time traces demonstrate the similar behavior due to the auxiliary ECRH. It is important to note that in earlier experiments, performed with higher densities [14] the opposite effect was observed by both correlation reflectometry and HIBP: QC mode was suppressed by ECRH. So, the details of the QC mode behavior under ECRH still present an open question.

The overall GAM frequency dependence on the electron temperature is presented in Fig. 10. Figure shows that despite the radially global character of GAM on T-10, which is inconsistent with the local theory [2], the GAM frequency follows the scalings (1 - 2) in the following sense: the frequency of the global eigenmode is driven by the sound speed c_s (Eq. (2)) taken at some representative radial point. This point happens to be $\rho = 0.7$ for all experimental points of Fig. 10. At the plasma edge $T_i \approx T_e$, [21], so the scaling for the GAM frequency may be rewritten as:

$$f_{\text{GAM}}^c = 1/2\pi R \sqrt{2T_e/m_i}. \quad (3)$$

It is shown by the solid line in Fig. 10.

4. Summary

The structure of the electrostatic turbulence in the ohmic plasmas of the T-10 tokamak is as follows:

There are two dominating modes in the power spectra: GAM (~ 20 kHz) and QC (50 - 150 kHz). GAM dom-

inates in plasma potential while QC dominates in the density spectra.

GAM has constant frequency and amplitude over the whole plasma column up to the periphery. Higher frequency satellite has the same structure, but it starts deeper in plasma.

SOL is characterized by a specific type of the spectra with strongly dominating low-frequency (< 20 kHz) band.

Both GAM and QC are affected by ECRH: GAM frequency increases with T_e due to ECRH, while GAM amplitude increases with ECRH. The dynamics of QC is more complicated. In contrast to the decrease of the QC under ECRH observed earlier [14], in the considered regimes QC were excited. In future, we plan to study the features of QC mode and GAM frequency scaling with account of T_i for ECRH discharges.

Acknowledgement

The study was performed due to the support of the Russian Science Foundation, project 14-22-00193.

- [1] P. Diamond *et al.*, Plasma Phys. Control. Fusion **47**, R35 (2005).
- [2] N. Winsor *et al.*, Phys. Fluids **11**, 2448 (1968).
- [3] A. Fujisawa *et al.*, Nucl. Fusion **47**, S718 (2007).
- [4] A.V. Melnikov *et al.*, Plasma Phys. Control. Fusion **48**, S87 (2006).
- [5] J. Seidl *et al.*, Nucl. Fusion **57**, 126048 (2017).
- [6] D. Basu *et al.*, Nucl. Fusion **58**, 024001 (2018).
- [7] G.D. Convey *et al.*, Plasma Phys. Control. Fusion **50**, 055009 (2008).
- [8] T. Ido *et al.*, Plasma Phys. Control. Fusion **48**, S41 (2006).
- [9] A.V. Melnikov *et al.*, Nucl. Fusion **55**, 063001 (2015).
- [10] A.D. Gurchenko *et al.*, Plasma Phys. Control. Fusion **55**, 085017 (2013).
- [11] A.V. Melnikov *et al.*, JETP Letters **100**, 555 (2014).
- [12] A.V. Melnikov *et al.*, Rev. Sci. Instrum. **66**, 317 (1995).
- [13] A.V. Melnikov *et al.*, Czech. J. Phys. **55**, 349 (2005).
- [14] V.A. Vershkov *et al.*, Nucl. Fusion **45**, S203 (2005).
- [15] V.A. Vershkov *et al.*, Nucl. Fusion **57**, 102017 (2017).
- [16] V.A. Krupin *et al.*, Nucl. Fusion **57**, 066041 (2017).
- [17] M.A. Drabinskij *et al.*, J. Phys.: Conf. Series **747**, 012017 (2016).
- [18] A.V. Melnikov *et al.*, Nucl. Fusion **57**, 072004 (2017).
- [19] L.G. Eliseev *et al.*, J. Phys.: Conf. Series **907**, 012002 (2017).
- [20] D.W. Ross *et al.*, Rev. Sci. Instrum. **63**, 2232 (1992).
- [21] L.A. Klyuchnikov *et al.*, Rev. Sci. Instrum. **87**, 053506 (2016).